Scaling Properties of Hyperon Production in Au+Au Collisions at √sNN=200 GeV

(STAR Collaboration) Adams, J.; ...; Planinić, Mirko; ...; Poljak, Nikola; ...; Zuo, J. X.

Scaling Properties of Hyperon Production in Au + Au Collisions at $\sqrt{s_{NN}} = 200$ GeV

J. Adams,[2] M. M. Aggarwal,[29] Z. Ahammed,[44] J. Amonett,[19] B. D. Anderson,[19] M. Anderson,[6] D. Arkhipkin,[12] G. S. Averichev,[11] Y. Bai,[27] J. Balewski,[16] O. Barannikova,[2] L. S. Barnby,[2] J. Baudot,[17] S. Bekele,[28] V. V. Belaga,[11] A. Bellingeri-Laurikainen,[39] R. Bellwied,[47] B. I. Bezverkhny,[49] S. Bhardwaj,[34] A. Bhasin,[18] A. K. Bhati,[29] H. Bichsel,[46] J. Bielcik,[49] J. Bielcikova,[49] L. C. Bland,[3] C. O. Blyth,[2] S-L. Blyth,[21] B. E. Bonner,[35] M. Botje,[27] J. Bouchet,[39] A. V. Brandin,[25] A. Bravar,[3] M. Bystersky,[10] R. V. Cadman,[1] X. Z. Cai,[38] H. Caines,[49] M. Calderón de la Barca Sánchez,[6] J. Castillo,[27] O. Catu,[49] D. Cebra,[6] Z. Chajecki,[28] P. Chaloupka,[10] S. Chattopadhyay,[44] H. F. Chen,[37] J. H. Chen,[38] Y. Chen,[7] J. Cheng,[42] M. Cherney,[9] A. Chikanian,[49] H. A. Choi,[33] W. Christie,[3] J. P. Coffin,[17] T. M. Cormier,[47] M. R. Cosentino,[36] J. G. Cramer,[46] H. J. Crawford,[5] D. Das,[44] S. Das,[44] M. Daugherity,[41] M. M. de Moura,[36] T. G. Dedovich,[11] M. DePhillips,[3] A. A. Derevschikov,[31] L. Didenko,[3] T. Dietel,[13] P. Djawotho,[16] S. M. Dogra,[18] W. J. Dong,[7] X. Dong,[37] J. E. Draper,[6] F. Du,[49] V. B. Dunin,[11] J. C. Dunlop,[3] M. R. Dutta Mazumdar,[44] V. Eckardt,[23] W. R. Edwards,[21] L. G. Efimov,[11] V. Emelianov,[25] J. Engelage,[5] G. Eppley,[35] B. Erazmus,[39] M. Estienne,[17] P. Fachini,[3] R. Fatemi,[22] J. Fedorisin,[11] K. Filimonov,[21] P. Filip,[12] E. Finch,[49] V. Fine,[3] Y. Fisyak,[3] J. Fu,[48] C. A. Gagliardi,[40] L. Gaillard,[2] J. Gans,[49] M. S. Ganti,[44] V. Ghazikhanian,[7] P. Ghosh,[44] J. E. Gonzalez,[7] Y. G. Gorbunov,[9] H. Gos,[45] O. Grebenyuk,[27] D. Grosnick,[43] S. M. Guertin,[7] K. S. F. F. Guimaraes,[36] Y. Guo,[47] N. Gupta,[18] T. D. Gutierrez,[6] B. Haag,[6] T. J. Hallman,[3] A. Hamed,[47] J. W. Harris,[49] W. He,[16] M. Heinz,[49] T. W. Henry,[40] S. Hepplemann,[30] B. Hippolyte,[17] A. Hirsch,[32] E. Hjort,[21] G. W. Hoffmann,[41] M. J. Horner,[21] H. Z. Huang,[7] S. L. Huang,[37] E. W. Hughes,[4] T. J. Humanic,[28] G. Igo,[7] P. Jacobs,[21] W. W. Jacobs,[16] P. Jakl,[10] F. Jia,[20] H. Jiang,[7] P. G. Jones,[2] E. G. Judd,[5] S. Kabana,[39] K. Kang,[42] J. Kapitan,[10] M. Kaplan,[8] D. Keane,[19] A. Kechechyan,[11] V. Yu. Khodyrev,[31] B. C. Kim,[33] J. Kiryluk,[22] A. Kisiel,[45] E. M. Kislov,[11] S. R. Klein,[21] D. D. Koetke,[43] T. Kollegger,[13] M. Kopytine,[19] L. Kotchenda,[25] V. Kouchpil,[10] K. L. Kowalik,[21] M. Kramer,[26] P. Kravtsov,[25] V. I. Kravtsov,[31] K. Krueger,[1] C. Kuhn,[17] A. I. Kulikov,[11] A. Kumar,[29] A. A. Kuznetsov,[11] M. A. C. Lamont,[49] J. M. Landgraf,[3] S. Lange,[13] S. LaPointe,[47] F. Laue,[3] J. Lauret,[3] A. Lebedev,[3] R. Lednicky,[12] C-H. Lee,[33] S. Lehocka,[11] M. J. LeVine,[3] C. Li,[37] Q. Li,[47] Y. Li,[42] G. Lin,[49] S. J. Lindenbaum,[26] M. A. Lisa,[28] F. Liu,[48] H. Liu,[37] J. Liu,[35] L. Liu,[48] Z. Liu,[48] T. Ljubicic,[3] W. J. Llope,[35] H. Long,[7] R. S. Longacre,[3] M. Lopez-Noriega,[28] W. A. Love,[3] Y. Lu,[50] T. Ludlam,[3] D. Lynn,[3] G. L. Ma,[38] J. G. Ma,[7] Y. G. Ma,[38] D. Magestro,[28] D. P. Mahapatra,[14] R. Majka,[49] L. K. Mangotra,[18] R. Manweiler,[43] S. Margetis,[19] C. Markert,[19] L. Martin,[39] H. S. Matis,[21] Yu. A. Matulenko,[31] C. J. McClain,[1] T. S. McShane,[9] Yu. Melnick,[31] A. Meschanin,[31] M. L. Miller,[22] N. G. Minaev,[31] S. Mioduszewski,[40] C. Mironov,[19] A. Mischke,[27] D. K. Mishra,[14] J. Mitchell,[35] B. Mohanty,[44] L. Molnar,[32] C. F. Moore,[41] D. A. Morozov,[31] M. G. Munhoz,[36] B. K. Nandi,[15] C. Nattrass,[49] T. K. Nayak,[44] J. M. Nelson,[2] P. K. Netrakanti,[44] V. A. Nikitin,[12] L. V. Nogach,[31] S. B. Nurushev,[31] G. Odyniec,[21] A. Ogawa,[3] V. Okorokov,[25] M. Oldenburg,[21] D. Olson,[21] M. Pachr,[10] S. K. Pal,[44] Y. Panebratsev,[11] S. Y. Panitkin,[3] A. I. Pavlinov,[47] T. Pawlak,[45] T. Peitzmann,[27] V. Perevoztchikov,[3] C. Perkins,[5] W. Peryt,[45] V. A. Petrov,[47] S. C. Phatak,[14] R. Picha,[6] M. Planinic,[50] J. Pluta,[45] N. Poljak,[50] N. Porile,[32] J. Porter,[46] A. M. Poskanzer,[21] M. Potekhin,[3] E. Potrebenikova,[11] B. V. K. S. Potukuchi,[18] D. Prindle,[46] C. Pruneau,[47] J. Putschke,[21] G. Rakness,[30] R. Raniwala,[34] S. Raniwala,[34] R. L. Ray,[41] S. V. Razin,[11] J. Reinnarth,[39] D. Relyea,[4] F. Retiere,[21] A. Ridiger,[25] H. G. Ritter,[21] J. B. Roberts,[35] O. V. Rogachevskiy,[11] J. L. Romero,[6] A. Rose,[21] C. Roy,[39] L. Ruan,[21] M. J. Russcher,[27] R. Sahoo,[14] I. Sakrejda,[21] S. Salur,[49] J. Sandweiss,[49] M. Sarsour,[40] P. S. Sazhin,[11] J. Schambach,[41] R. P. Scharenberg,[32] N. Schmitz,[23] K. Schweda,[21] J. Seger,[9] I. Selyuzhenkov,[47] P. Seyboth,[23] A. Shabetai,[21] E. Shahaliev,[11] M. Shao,[37] M. Sharma,[29] W. Q. Shen,[38] S. S. Shimanskiy,[11] E Sichtermann,[21] F. Simon,[22] R. N. Singaraju,[44] N. Smirnov,[49] R. Snellings,[27] G. Sood,[43] P. Sorensen,[3] J. Sowinski,[16] J. Speltz,[17] H. M. Spinka,[1] B. Srivastava,[32] A. Stadnik,[11] T. D. S. Stanislaus,[43] R. Stock,[13] A. Stolpovsky,[47] M. Strikhanov,[25] B. Stringfellow,[32] A. A. P. Suaide,[36] E. Sugarbaker,[28] M. Sumbera,[10] Z. Sun,[20] B. Surrow,[22] M. Swanger,[9] T. J. M. Symons,[21] A. Szanto de Toledo,[36] A. Tai,[7] J. Takahashi,[36] A. H. Tang,[3] T. Tarnowsky,[32] D. Thein,[7] J. H. Thomas,[21] A. R. Timmins,[2] S. Timoshenko,[25] M. Tokarev,[11] T. A. Trainor,[46] S. Trentalange,[7] R. E. Tribble,[40] O. D. Tsai,[7] J. Ulery,[32] T. Ullrich,[3] D. G. Underwood,[1] G. Van Buren,[3] N. van der Kolk,[27] M. van Leeuwen,[21] A. M. Vander Molen,[24] R. Varma,[15] I. M. Vasilevski,[12] A. N. Vasiliev,[31] R. Vernet,[17] S. E. Vigdor,[16] Y. P. Viyogi,[44] S. Vokal,[11] S. A. Voloshin,[47] W. T. Waggoner,[9] F. Wang,[32] G. Wang,[19] J. S. Wang,[20] X. L. Wang,[37] Y. Wang,[42] J. W. Watson,[19] J. C. Webb,[16] G. D. Westfall,[24] A. Wetzler,[21] C. Whitten, Jr.,[7] H. Wieman,[21] S. W. Wissink,[16] R. Witt,[49] J. Wood,[7] J. Wu,[37] N. Xu,[21] Q. H. Xu,[21] Z. Xu,[3] P. Yepes,[35] I-K. Yoo,[33] V. I. Yurevich,[11] W. Zhan,[20] H. Zhang,[3] W. M. Zhang,[19] Y. Zhang,[37] Z. P. Zhang,[37] Y. Zhao,[37] C. Zhong,[38] R. Zoulkarneev,[12] Y. Zoulkarneeva,[12] A. N. Zubarev,[11] and J. X. Zuo[38]

(STAR Collaboration)

[1]*Argonne National Laboratory, Argonne, Illinois 60439, USA*
[2]*University of Birmingham, Birmingham, United Kingdom*
[3]*Brookhaven National Laboratory, Upton, New York 11973, USA*
[4]*California Institute of Technology, Pasadena, California 91125, USA*
[5]*University of California, Berkeley, California 94720, USA*
[6]*University of California, Davis, California 95616, USA*
[7]*University of California, Los Angeles, California 90095, USA*
[8]*Carnegie Mellon University, Pittsburgh, Pennsylvania 15213, USA*
[9]*Creighton University, Omaha, Nebraska 68178, USA*
[10]*Nuclear Physics Institute AS CR, 250 68 Řež/Prague, Czech Republic*
[11]*Laboratory for High Energy (JINR), Dubna, Russia*
[12]*Particle Physics Laboratory (JINR), Dubna, Russia*
[13]*University of Frankfurt, Frankfurt, Germany*
[14]*Institute of Physics, Bhubaneswar 751005, India*
[15]*Indian Institute of Technology, Mumbai, India*
[16]*Indiana University, Bloomington, Indiana 47408, USA*
[17]*Institut de Recherches Subatomiques, Strasbourg, France*
[18]*University of Jammu, Jammu 180001, India*
[19]*Kent State University, Kent, Ohio 44242, USA*
[20]*Institute of Modern Physics, Lanzhou, China*
[21]*Lawrence Berkeley National Laboratory, Berkeley, California 94720, USA*
[22]*Massachusetts Institute of Technology, Cambridge, Massachusetts 02139-4307, USA*
[23]*Max-Planck-Institut für Physik, Munich, Germany*
[24]*Michigan State University, East Lansing, Michigan 48824, USA*
[25]*Moscow Engineering Physics Institute, Moscow Russia*
[26]*City College of New York, New York, New York 10031, USA*
[27]*NIKHEF and Utrecht University, Amsterdam, The Netherlands*
[28]*Ohio State University, Columbus, Ohio 43210, USA*
[29]*Panjab University, Chandigarh 160014, India*
[30]*Pennsylvania State University, University Park, Pennsylvania 16802, USA*
[31]*Institute of High Energy Physics, Protvino, Russia*
[32]*Purdue University, West Lafayette, Indiana 47907, USA*
[33]*Pusan National University, Pusan, Republic of Korea*
[34]*University of Rajasthan, Jaipur 302004, India*
[35]*Rice University, Houston, Texas 77251, USA*
[36]*Universidade de Sao Paulo, Sao Paulo, Brazil*
[37]*University of Science and Technology of China, Hefei 230026, China*
[38]*Shanghai Institute of Applied Physics, Shanghai 201800, China*
[39]*SUBATECH, Nantes, France*
[40]*Texas A&M University, College Station, Texas 77843, USA*
[41]*University of Texas, Austin, Texas 78712, USA*
[42]*Tsinghua University, Beijing 100084, China*
[43]*Valparaiso University, Valparaiso, Indiana 46383, USA*
[44]*Variable Energy Cyclotron Centre, Kolkata 700064, India*
[45]*Warsaw University of Technology, Warsaw, Poland*
[46]*University of Washington, Seattle, Washington 98195, USA*
[47]*Wayne State University, Detroit, Michigan 48201, USA*
[48]*Institute of Particle Physics, CCNU (HZNU), Wuhan 430079, China*
[49]*Yale University, New Haven, Connecticut 06520, USA*
[50]*University of Zagreb, Zagreb, HR-10002, Croatia*

(Received 8 June 2006; published 5 February 2007)

We present the scaling properties of Λ, Ξ, and Ω in midrapidity Au + Au collisions at the Brookhaven National Laboratory Relativistic Heavy Ion Collider at $\sqrt{s_{NN}} = 200$ GeV. The yield of multistrange baryons per participant nucleon increases from peripheral to central collisions more rapidly than that of Λ, indicating an increase of the strange-quark density of the matter produced. The strange phase-space occupancy factor γ_s approaches unity for the most central collisions. Moreover, the nuclear modification factors of p, Λ, and Ξ are consistent with each other for $2 < p_T < 5$ GeV/c in agreement with a scenario of hadron formation from constituent quark degrees of freedom.

DOI: 10.1103/PhysRevLett.98.062301 PACS numbers: 25.75.Dw

Lattice QCD calculations predict that a new state of matter, the quark gluon plasma (QGP), can be formed in nuclear collisions when the temperature exceeds 170 MeV [1]. Strange quarks, whose mass is comparable to the critical temperature, are expected to be abundantly produced by thermal parton interactions in the high temperature QGP phase. Because of the corresponding increase in the strange-quark density, hyperon production is expected to be enhanced in high energy nuclear collisions with respect to $p + p$ or $p + A$ collisions, the enhancement increasing with the number of strange quarks in the hyperon [2]. Such an effect has already been observed in various fixed-target experiments at lower energy [3–5]. In this Letter, we study the centrality dependence of hyperon production in Au + Au collisions at $\sqrt{s_{NN}} = 200$ GeV, an order of magnitude higher than that previously achieved. We also study the transverse momentum dependence of hyperon production in central and peripheral collisions in an attempt to shed light upon the possible production mechanisms.

Previous studies have shown that ratios of hadron yields in high energy $A + A$ collisions are generally well described by statistical models in the grand-canonical limit [6–8]. A strangeness phase-space occupancy factor γ_s is sometimes introduced to describe the extent to which strangeness reaches its equilibrium abundance. In this framework, the amount of strangeness produced per participating nucleon (N_{part}) is directly related to the value of γ_s. The centrality dependence of γ_s therefore provides a quantitative measure of strangeness equilibration as a function of system size in $A + A$ collisions [9], provided that canonical effects are small.

By contrast, at high transverse momentum, hadrons are thought to be produced via incoherent hard scatterings, which, in the absence of any nuclear medium effects, should scale with the number of binary nucleon-nucleon collisions (N_{bin}). Measurements of hadron production in Au + Au collisions at the Brookhaven National Laboratory Relativistic Heavy Ion Collider (RHIC) have shown that not only is there a deviation from binary scaling in central collisions [10,11] but also a distinct difference in the scaling behavior of baryons and mesons in the transverse momentum range $2 < p_T < 5$ GeV/c [12,13]. A strong particle-type dependence is not predicted by conventional Monte Carlo (MC) event simulators such as HIJING, where hadron formation in this region is dominated by independent parton fragmentation [14]. On the other hand, quark recombination (coalescence) models have been successful in explaining the observed deviation from binary scaling for baryons and mesons in central collisions [15–18], as well as providing an explanation for the particle-type dependence of measured azimuthal anisotropies at intermediate p_T in noncentral collisions [13]. By extending these studies to include multistrange baryons, we provide a more stringent test of such models. In the following, N_{part} and N_{bin} have been extracted from a MC Glauber calculation [11,19].

The STAR Time Projection Chamber (TPC) measures the trajectories and momenta of charged particles produced in each collision in the pseudorapidity range $|\eta| < 1.8$ [20]. The detector operates within a solenoidal magnetic field of 0.5 Tesla whose axis is aligned with the beam. A central trigger barrel, covering the pseudorapidity region $|\eta| < 1$, and two zero-degree calorimeters are used as trigger detectors. From a total of 1.6×10^6 minimum-bias and 1.5×10^6 central trigger collisions analyzed, five centrality bins were selected corresponding to the following ranges in the total hadronic cross section: 0%–5%, 10%–20%, 20%–40%, 40%–60%, and 60%–80%. The collision centrality was defined by the charged particle multiplicity measured in the TPC in the pseudorapidity range $|\eta| < 0.5$. The 0%–5% bin was obtained from the central trigger sample. The remaining bins were obtained from the minimum-bias sample. Because of relatively poor statistics, the 5%–10% bin was omitted from this analysis.

$\Lambda(\bar{\Lambda})$, $\Xi^-(\bar{\Xi}^+)$, and $\Omega^-(\bar{\Omega}^+)$ were reconstructed from their charged decay modes in the TPC, in rapidity intervals of $|y| < 1$, 0.75, and 0.75, respectively. The signal was extracted by plotting invariant mass distributions for each particle in bins of transverse momentum and centrality. Topological cuts were applied to reduce combinatorial background and to obtain a well-behaved (linear) background in the vicinity of the mass peak. The statistics of Ω^- and $\bar{\Omega}^+$ have been combined in order to obtain p_T distributions in 3 of the 5 centrality bins. The average signal to background ratio in the 0%–5% centrality bin (worst case) was 5 for Λ, 1.4 for Ξ, and 2 for $\Omega^- + \bar{\Omega}^+$. After background subtraction, corrections were applied for detector acceptance and reconstruction efficiency. The efficiency calculations were based on the probability of finding Monte Carlo generated particles after processing them through a TPC detector response simulation and embedding them into real events. A detailed description of the analysis can be found elsewhere [21–23].

Figure 1 shows the transverse momentum distributions of $\Lambda(\bar{\Lambda})$, $\Xi^-(\bar{\Xi}^+)$, and $\Omega^- + \bar{\Omega}^+$ measured at midrapidity and as a function of centrality. The Λ spectra were corrected for feed-down from multistrange baryon weak decays, based upon the measured Ξ and Ω spectra. The contribution to the Λ spectrum from Ξ, Ξ^0, and Ω decays was around 15%, while the feed-down contribution to the Ξ spectrum from Ω decays was negligible. The total integrated yields (dN/dy) presented in Table I were extracted from Boltzmann fits to the spectra. The measured p_T coverage is about 70% of the total Λ yield and 60% for Ξ and Ω.

The systematic error on the reconstructed yields was studied as a function of p_T. Three main factors contribute

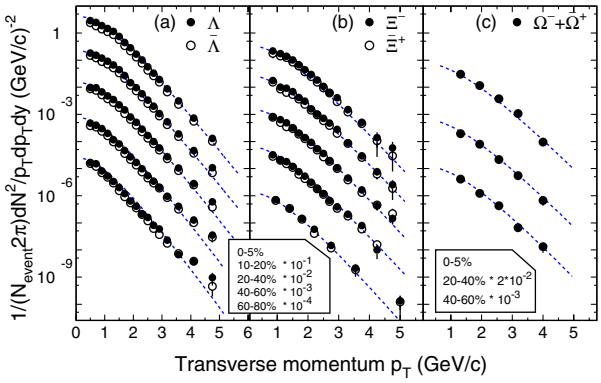

FIG. 1 (color online). Transverse momentum distributions of (a) $\Lambda(\bar{\Lambda})$ for $|y| < 1.0$, (b) $\Xi^-(\bar{\Xi}^+)$ for $|y| < 0.75$, and (c) $\Omega^- + \bar{\Omega}^+$ for $|y| < 0.75$ in Au + Au collisions at $\sqrt{s_{NN}} = 200$ GeV as a function of centrality. Scale factors were applied to the spectra for clarity. Only statistical errors are shown. The dashed curves show a Boltzmann fit to the Λ, Ξ^-, and $\Omega^- + \bar{\Omega}^+$ data; the fits to the $\bar{\Lambda}$ and $\bar{\Xi}^+$ are omitted for clarity.

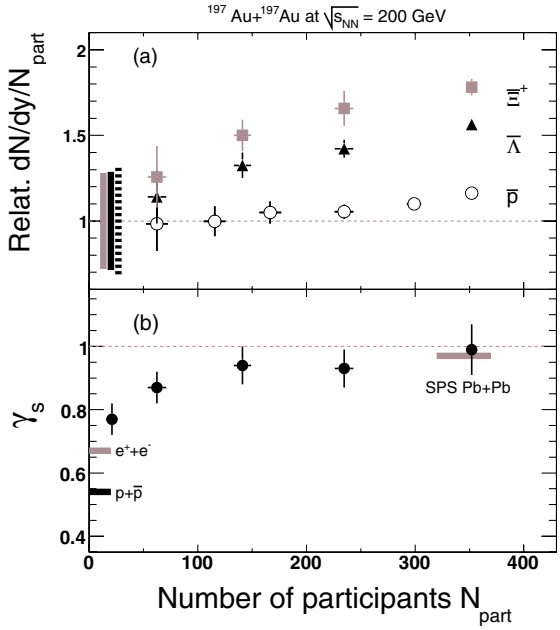

FIG. 2 (color online). (a) The integrated yield dN/dy at midrapidity for $\bar{\Xi}^+$, $\bar{\Lambda}$, and $\bar{p}$ divided by N_{part}, normalized to the most peripheral collisions (60%–80%), plotted as a function of N_{part}. The gray, black, and dashed bands represent the errors on the normalization to the bin 60%–80% for $\bar{\Xi}^+$, $\bar{\Lambda}$, and $\bar{p}$, respectively. Other errors shown are statistical only. (b) γ_s as a function of N_{part} for Au + Au collisions at 200 GeV (cf. text for details). Values for $e^+ + e^-$, $p + \bar{p}$, and Pb + Pb collisions at $\sqrt{s_{NN}} = 91$, 200, and 17.2 GeV, respectively, are shown for comparison [26–28].

to this error: (i) subtle differences between the MC simulation and real data, which make the reconstructed yields sensitive to the choice of topological cuts, (ii) sensitivity to the method used to subtract the remaining background after cuts have been applied, and (iii) measured differences in the yield dependent on the direction of the applied magnetic field. The systematic uncertainty on the fit parameters was determined by adding p_T dependent systematic errors to the data points shown in Fig. 1 and performing a second fit. We also investigated the choice of function used to fit the data. Although the Boltzmann function gave a better fit, an exponential shape could not be excluded. Exponential fits to the data gave a 5%–6% higher yield on average and a larger inverse slope parameter by 40–50 MeV. These differences are not included in the errors shown in Table I.

Figure 2(a) presents the strange antiparticle yields dN/dy divided by N_{part}. All data points are normalized to the values obtained in the most peripheral collisions. The centrality dependence of the antiproton yield is also shown for comparison [24]. Strange antiparticles are chosen because all valence quarks must have been created in the collision, although similar results are also obtained for strange particles. In a geometrical description of nuclear collisions, the number of participant nucleons is proportional to the initial overlapping volume of the colliding nuclei. The integrated yield is dominated by the low p_T

TABLE I. Integrated yields dN/dy and inverse slope parameters T (MeV) extracted from a Boltzmann fit to the p_T spectra of $\Lambda(\bar{\Lambda})$, $\Xi^-(\bar{\Xi})^+$, and $\Omega^- + \bar{\Omega}^+$ at midrapidity, with their statistical and systematic errors. $\langle N_{\text{part}} \rangle$ is shown for each centrality.

Centrality	0%–5%	10%–20%	20%–40%	40%–60%	60%–80%
$\langle N_{\text{part}} \rangle$	352 ± 3	235 ± 9	141 ± 8	62 ± 9	21 ± 6
Λ	$16.7 \pm 0.2 \pm 1.1$	$10.0 \pm 0.1 \pm 0.7$	$5.53 \pm 0.05 \pm 0.39$	$2.07 \pm 0.03 \pm 0.14$	$0.58 \pm 0.01 \pm 0.04$
	$309 \pm 1 \pm 8$	$308 \pm 1 \pm 8$	$303 \pm 1 \pm 8$	$297 \pm 2 \pm 10$	$287 \pm 3 \pm 10$
$\bar{\Lambda}$	$12.7 \pm 0.2 \pm 0.9$	$7.7 \pm 0.1 \pm 0.5$	$4.30 \pm 0.04 \pm 0.30$	$1.64 \pm 0.03 \pm 0.11$	$0.48 \pm 0.01 \pm 0.03$
	$310 \pm 1 \pm 7$	$309 \pm 1 \pm 8$	$306 \pm 1 \pm 9$	$298 \pm 2 \pm 10$	$282 \pm 3 \pm 10$
Ξ^-	$2.17 \pm 0.06 \pm 0.19$	$1.41 \pm 0.04 \pm 0.08$	$0.72 \pm 0.02 \pm 0.02$	$0.26 \pm 0.01 \pm 0.02$	$0.063 \pm 0.004 \pm 0.003$
	$335 \pm 4 \pm 7$	$331 \pm 4 \pm 8$	$326 \pm 3 \pm 6$	$325 \pm 4 \pm 7$	$320 \pm 8 \pm 13$
$\bar{\Xi}^+$	$1.83 \pm 0.05 \pm 0.20$	$1.14 \pm 0.04 \pm 0.08$	$0.62 \pm 0.02 \pm 0.03$	$0.23 \pm 0.01 \pm 0.02$	$0.061 \pm 0.004 \pm 0.002$
	$335 \pm 4 \pm 9$	$334 \pm 4 \pm 9$	$327 \pm 3 \pm 6$	$327 \pm 5 \pm 7$	$302 \pm 8 \pm 16$
$\Omega + \bar{\Omega}^+$	$0.53 \pm 0.04 \pm 0.04$	$\cdots$	$0.17 \pm 0.02 \pm 0.01$	$0.063 \pm 0.008 \pm 0.004$	$\cdots$
	$353 \pm 9 \pm 10$	$\cdots$	$348 \pm 15 \pm 12$	$336 \pm 17 \pm 13$	$\cdots$

region, where particle production is driven mainly by soft processes. The yield per participating nucleon may reflect the formation probability of a hadron from the bulk. We would then expect it to be sensitive to the density of the hadron's constituent quarks in the system. We note that there appears to be a hierarchy of particle production dependent upon strange-quark content.

Thermal-statistical models have been successful in describing particle yields in various systems at different energies [6,7]. The possible nonequilibrium of strange quarks is taken into account by introducing a phase-space occupancy factor γ_s. With the measured midrapidity yields of strange baryons, of pions, kaons, protons, and their antiparticles [24], we have performed a fit using the model described in Ref. [25] to determine γ_s as a function of N_{part}, as shown in Fig. 2(b). Within the grand-canonical framework, we find that the value of γ_s increases from about 0.8 in peripheral collisions to about 1.0 in central collisions. In each case, we obtained a freeze-out temperature around 165 MeV. According to the model, the Λ yield depends linearly on γ_s, while the yield of Ξ depends on γ_s^2, consistent with the behavior observed in Fig. 2(a). The fact that γ_s approaches unity when $N_{\text{part}} > 150$ suggests that the strange-quark abundance tends to equilibrate as the system size increases. Also shown in Fig. 2(b) is the result of a recent analysis of hadron yields in $A + A$ collisions at $\sqrt{s_{NN}} = 17.2$ GeV, which also found that $\gamma_s \approx 1$ at midrapidity in central collisions [26], while in elementary $e + e$ and $p + \bar{p}$ collisions at various energies γ_s was found to be significantly less than unity [27,28].

We studied the effect of including different combinations of particles in the fit and found that particle ratios involving protons and Λ are important in constraining the freeze-out temperature and γ_s, respectively. The value and centrality dependence of γ_s is relatively insensitive to the inclusion of other particle ratios in the fit. The errors shown in Fig. 2(b) reflect the variation of γ_s found in this study. Since the most peripheral bin corresponds to events with an average number of 20 participants, we anticipate canonical effects to be small [29]. However, a more recent study suggests that canonical effects may persist over a wider range of participants [30], which may provide an alternative explanation for the centrality dependence shown in Fig. 2(a).

Figure 3 shows the nuclear modification factor (R_{CP}) [13] for $\Xi^- + \bar{\Xi}^+$ and $\Omega + \bar{\Omega}$. It was found by forming the ratio of the p_T spectra of the 0%–5% and 40%–60% centrality bins, after normalizing each spectrum to the appropriate average number of binary collisions. The 40%–60% centrality bin was chosen as the reference because of the limited statistics of $\Omega + \bar{\Omega}$ in the 60%–80% bin. Also shown in Fig. 3 are the previously published results for charged hadrons and $\Lambda + \bar{\Lambda}$ for the same centrality bins [13]. The dark gray rectangular boxes represent the expected R_{CP} range for N_{part} and N_{bin} scalings, indicating the range of uncertainty in their calculation. Although

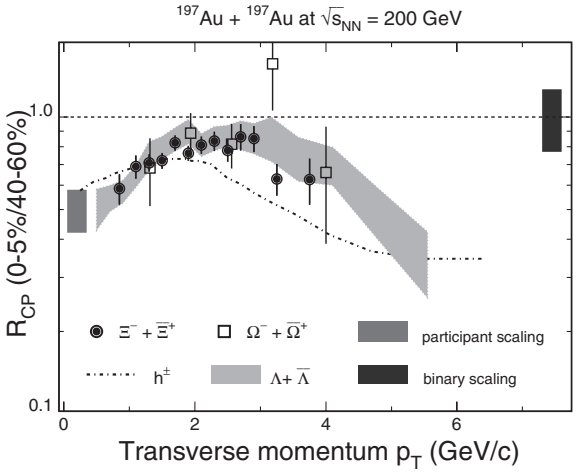

FIG. 3. R_{CP} for $\Xi^- + \bar{\Xi}^+$ and $\Omega^- + \bar{\Omega}^+$ at midrapidity (0%–5% vs 40%–60%). A dashed line for charged hadrons and a gray band for $\Lambda + \bar{\Lambda}$ are shown for comparison. The gray rectangles represent participant and binary scalings.

the p_T integrated yield per participating nucleon of Ξ increases faster with N_{part} than for Λ hyperons, in the interval $1.8 < p_T < 3.5$ GeV/c, the p_T dependences of R_{CP} for $\Xi^- + \bar{\Xi}^+$ and $\Omega^- + \bar{\Omega}^+$ are similar and coincide with the trend previously shown for $\Lambda + \bar{\Lambda}$. The R_{CP} of hyperons exhibits little suppression, while mesons (approximated by the dashed line) have a distinctly different trend. The difference in R_{CP} for baryons and mesons in the intermediate p_T region has previously been discussed in the framework of recombination (or coalescence) models [10,13,17,31]. The results presented here appear to confirm that the difference is dependent upon the number of constituent quarks rather than mass. Further weight is given to this argument by a recent measurement of the R_{CP} of protons [12], $K(892)^*$ [32], and ϕ mesons [33]. Futhermore, it suggests that the strange-quark distribution scales with centrality similarly to u and d quarks, since baryons with different strangeness content seem to follow the same pattern.

In this Letter, we have presented the scaling properties of strange baryon production in Au + Au collisions at $\sqrt{s_{NN}} = 200$ GeV. By studying the hyperon yields scaled by N_{part} and the centrality dependence of γ_s within the framework of a thermal model, we have found that strangeness equilibrium appears to have been achieved in central collisions at RHIC. Investigating the centrality dependence of the p_T distributions of hyperons, we find that their yields in central collisions fall below the expectation for binary scaling for $p_T > 3$ GeV/c and that, within the error bars, the nuclear modification factor R_{CP} is similar for all baryons independent of their mass or strangeness content. This feature is consistent with models of hadron formation based upon quark recombination.

We thank the RHIC Operations Group and RCF at BNL and the NERSC Center at LBNL for their support. This work was supported in part by the Offices of NP and HEP

within the U.S. DOE Office of Science; the U.S. NSF; the BMBF of Germany; IN2P3, RA, RPL, and EMN of France; EPSRC of the United Kingdom; FAPESP of Brazil; the Russian Ministry of Science and Technology; the Ministry of Education and the NNSFC of China; IRP and GA of the Czech Republic; FOM of the Netherlands; DAE, DST, and CSIR of the Government of India; Swiss NSF; the Polish State Committee for Scientific Research; SRDA of Slovakia; and the Korea Science and Engineering Foundation.

[1] Z. Fodor and S. D. Katz, J. High Energy Phys. 04 (2004) 050.
[2] J. Rafelski and B. Muller, Phys. Rev. Lett. **48**, 1066 (1982).
[3] E. Andersen *et al.* (WA97 Collaboration), Phys. Lett. B **449**, 401 (1999).
[4] C. Blume *et al.* (NA49 Collaboration), Nucl. Phys. **A698**, 104 (2002).
[5] F. Antinori *et al.* (NA57 Collaboration), J. Phys. G **32**, 427 (2006).
[6] P. Braun-Munzinger *et al.*, Phys. Lett. B **518**, 41 (2001).
[7] J. Rafelski and J. Letessier, Nucl. Phys. **A715**, 98 (2003).
[8] F. Becattini and L. Ferroni, Eur. Phys. J. C **38**, 225 (2004).
[9] J. Cleymans, B. Kaempfer, P. Steinberg, and S. Wheaton, J. Phys. G **30**, S595 (2004).
[10] K. Adcox *et al.* (PHENIX Collaboration), Phys. Rev. Lett. **88**, 022301 (2001).
[11] C. Adler *et al.* (STAR Collaboration), Phys. Rev. Lett. **89**, 202301 (2002).
[12] S. S. Adler *et al.* (PHENIX Collaboration), Phys. Rev. C **69**, 034909 (2004); J. Adams *et al.* (STAR Collaboration), Phys. Rev. Lett. **97**, 152301 (2006).
[13] J. Adams *et al.* (STAR Collaboration), Phys. Rev. Lett. **92**, 052302 (2004).
[14] B. Andersson *et al.*, Phys. Rep. **97**, 31 (1983), and references therein.
[15] D. Molnar and S. A. Voloshin, Phys. Rev. Lett. **91**, 092301 (2003).
[16] Z. W. Lin and C. M. Ko, Phys. Rev. Lett. **89**, 202302 (2002).
[17] R. J. Fries *et al.*, Phys. Rev. C **68**, 044902 (2003).
[18] V. Greco, C. M. Ko, and P. Levai, Phys. Rev. C **68**, 034904 (2003).
[19] R. J. Glauber, in *Lectures Delivered at the Summer Institute for Theoretical Physics, University of Colorado, Boulder, 1958*, edited by W. E. Brittin and L. G. Dunham, Lectures in Theoretical Physics Vol. 1 (Interscience, New York, 1959), pp. 315–414.
[20] M. Anderson *et al.* (STAR Collaboration), Nucl. Instrum. Methods Phys. Res., Sect. A **499**, 659 (2003).
[21] K. H. Ackermann *et al.* (STAR Collaboration), Phys. Rev. Lett. **86**, 402 (2001).
[22] C. Adler *et al.* (STAR Collaboration), Phys. Rev. Lett. **89**, 092301 (2002).
[23] J. Adams *et al.* (STAR Collaboration), Phys. Rev. Lett. **92**, 182301 (2004).
[24] J. Adams *et al.* (STAR Collaboration), Phys. Rev. Lett. **92**, 112301 (2004).
[25] J. Cleymans *et al.*, Phys. Rev. C **71**, 054901 (2005).
[26] F. Becattini *et al.*, Phys. Rev. C **69**, 024905 (2004).
[27] F. Becattini, Z. Phys. C **69**, 485 (1996).
[28] F. Becattini and U. Heinz, Z. Phys. C **76**, 269 (1997).
[29] K. Redlich and A. Tounsi, Eur. Phys. J. C **24**, 589 (2002).
[30] C. Höhne, F. Puhlhofer, and R. Stock, Phys. Lett. B **640**, 96 (2006).
[31] R. C. Hwa and C. B. Yang, Phys. Rev. C **67**, 034902 (2003).
[32] J. Adams *et al.* (STAR Collaboration), Phys. Rev. C **71**, 064902 (2005).
[33] J. Adams *et al.* (STAR Collaboration), Phys. Lett. B **612**, 181 (2005).